Active Response of the Structure beneath Japan due to Static and Dynamic Stress Changes from Large Earthquakes in 2003

Masatoshi MIYAZAWA* and James J. MORI

* COE Researcher, DPRI, Kyoto University

Synopsis

In order to monitor the crust and upper mantle beneath Japan, we investigate the active response to large earthquakes in 2003. The earthquake off the coast of Miyagi prefecture on 26 May (Mw 7.0) triggered local earthquakes in the Tohoku region due to static stress perturbations. The 2003 Tokachi-oki earthquake (Mw 8.3) on 26 September statically triggered the shallow earthquakes in the central Hokkaido and dynamically deep low frequency tremor at distances of more than 1000 km. We suggest seismic approaches using the z-value and statistic β value to illustrate the active response for the observed waveforms at Hi-net stations.

Keywords: active response, static triggering, dynamic triggering,
2003 Tokachi-oki earthquake

1. Introduction

After the occurrence of large earthquakes, seismic and volcanic events are often excited by stress changes and/or perturbations in the crust associated with the events (Harris, 1998). The excitation includes static and dynamic triggering of earthquakes, where the threshold for the stress condition to rupture a fault is exceeded. Permanent stress changes caused by a large earthquake can trigger nearby earthquakes, which is called "static triggering". Transient stress changes from the source propagate through the crust as seismic waves and are able to remotely trigger events, which is called "dynamic triggering".

Static triggering is usually observed within a few fault lengths from the main event, and is explained by Coulomb failure stress changes (ΔCFF). For example, Hashimoto (1995) reported the increases of seismic activity on the Tanba Plateau after the 1995 Kobe earthquake and Toda et al. (2001) argued that the western Tottori-ken earthquake in 2000 triggered the group of offset aftershocks, located about 25 km WSW from the main fault.

Investigation of active responses to static stress changes is restricted to a local area within a few fault lengths. However, we can study the active response over all of Japan, with the use of seismic waves from large earthquakes, which cause transient stress perturbations and possible dynamic triggering. Miyazawa (2002) showed that the dynamic triggering of volcanic tremor at Aso had a relation to the activity of the volcano, and the dynamic triggering reflects the current state of the volcano. However, the meaning of the active response in non-volcanic areas is not yet clear.

The deformation of the crust has been well studied by geodetic methods (e.g., GPS and strain meters), but the time-scale is generally not shorter than a few months or a few weeks, with the exception of large coseismic changes associated with the large earthquakes. The use of seismicity changes is another possible method to detect the changes in

the crust (e.g., Habermann, 1983; Reasenberg and Simpson, 1992), however, recognizing changes in seismicity patterns also usually take long observation periods. This long time-scale makes it difficult to detect precursory events immediately before large earthquakes on the time scale of a few days to a few hours.

If the relationship between the activity in the crust or upper mantle and the dynamic triggering is clear, as for the case of volcanoes, the monitoring of the dynamic triggering would provide information about the present state of the structure, because the dynamic triggering could be detected within a few hours. We suggest a new seismic method to detect dynamic triggering which would occur on short time scales by use of continuous seismic waveforms when

some large earthquakes occur.

In the present study, we illustrate the triggered events in the crust and upper mantle beneath Japan from the Mw 7.0 earthquake off the coast of Miyagi prefecture on 26 May 2003 (hereafter, called the Miyagi-oki earthquake) and the 2003 Tokachi-oki earthquake (Mw 8.3) to compare the static stress change (the spatial pattern of ΔCFF) with the changes of seismic activity, to evaluate the active response of the crust. For the 2003 Tokachi-oki earthquake, the detection of dynamic triggering makes it possible to monitor the active response over most of the main part of Japan.
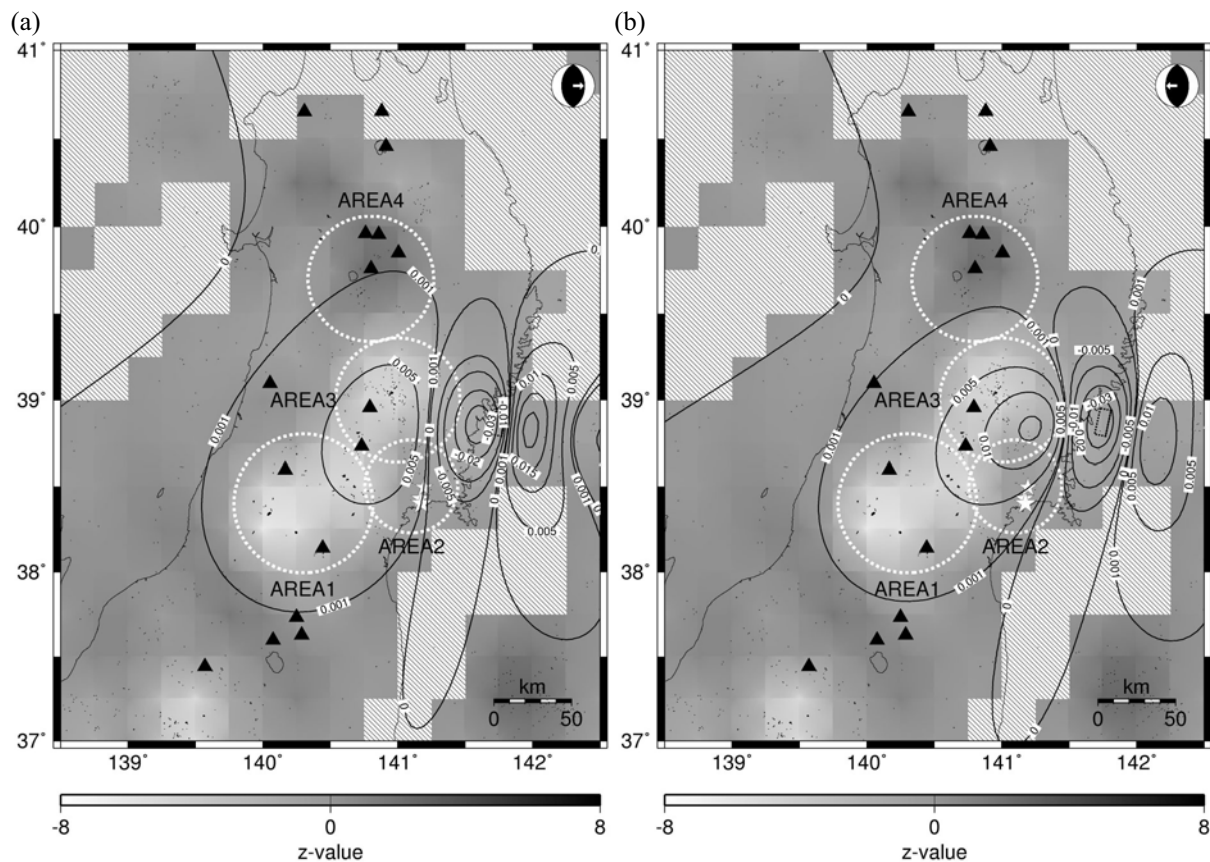

Fig. 1 Z-values estimated from shallow earthquakes (depth ≤ 20 km) of magnitude 0 to 5. Rectangular is the fault plane of the Miyagi-oki event on May 26, 2003. The two time windows used for calculating z-values are March 26 to May 25 and May 26 to July 25, which correspond to the pre- and post-seismic periods, respectively. Negative values in the bright areas indicate increases of activity and positive values in the dark areas decreases. Triangles are active volcanoes and dots are the hypocenters of the shallow earthquakes during the post-seismic period. Contour lines in (a) and (b) show the ΔCFF values in MPa calculated for a depth of 10 km, for two possible types of faults of the triggered seismicity. Both orientations have NS strikes and (a) has eastward dipping faults and (b) westward dipping, as illustrated by the stereoplots in the upper right of each figure. Stars are hypocenters of a sequence of moderate earthquakes (M_{JMA} 5.6, 6.2, 5.4) on July 26, 2003.

2. Triggering from the 2003 Miyagi-oki earthquake

We investigate the relationship between static stress changes due to the 2003 Miyagi-oki earthquake (Mw 7.0) and changes of seismicity around the Tohoku region, by evaluating the Coulomb failure function change (ΔCFF) and the z-value.

ΔCFF is expressed as

$$\Delta \mathrm{CFF} = \Delta \tau + \mu' \Delta \sigma_n \qquad (1)$$

where $\Delta \tau$ is the shear stress change across a fault in the area of interest and takes positive value if the increase is in the same direction as the slip, μ' is the apparent coefficient of friction including pore pressure effects, and $\Delta \sigma_n$ is the normal stress change and positive for traction across the fault.

Some fault models of this earthquake have been determined by the National Research Institute for Earth Science and Disaster Prevention (NIED), the Japan Meteorological Agency (JMA) and the Geographical Survey Institute (GSI) (the coordinating committee for earthquake prediction Japan (CCEP), 2004). The models of NIED and JMA were determined using seismic waveform data and the GSI model used GPS data. To calculate static stress changes, it is probably better to use a model obtained from geodetic data, so we adopt parameters mainly from the GSI model. We assume a simple rectangular fault plane (19 km × 17 km), where the slip is uniform, and choose the other parameters as follows. The northeastern corner of the fault is located at 38.94N, 141.81E, the depth of the top of the fault is 52 km, strike = 192 deg, dip = 68 deg, rake = 73 deg, and slip = 2.1 m. We also assume $\mu' = 0.4$ and the rigidity = 40 GPa. Spatial stress changes due to the earthquake are calculated by the method of Okada (1992). The orientation of fault planes on which the static stress changes are evaluated is assumed to have a NS strike and dip of 45 deg (i.e. NS-reverse fault) because the Tohoku region is under EW compression from the subducting Pacific plate and most earthquakes in this region have this type of focal mechanism. We also tried other fault models, however the pattern of ΔCFF is similar and the differences are not significant at far distances.

Changes of seismicity are statistically evaluated by the z-value (Habermann, 1983),

$$z = \frac{m_1 - m_2}{\sqrt{\sigma_1^2 / n_1 - \sigma_2^2 / n_2}} \qquad (2)$$

where, in an arbitrary time-window, n is the total number of earthquakes, m is the mean number of events in the time unit (one day), σ is the standard deviation, and suffixes 1 and 2 stand for "pre-seismic" and "post-seismic", respectively. When seismicity increases and decreases after the occurrence of the main earthquake, the z-value has negative and positive values, respectively. In this study we use time-windows of two months before and after May 26, 2003 when the Miyagi-oki earthquake occurred. In the pre- and post-seismic periods, the analyzed earthquakes from JMA data have magnitudes of M0 to M5 and depths shallower than 20 km.
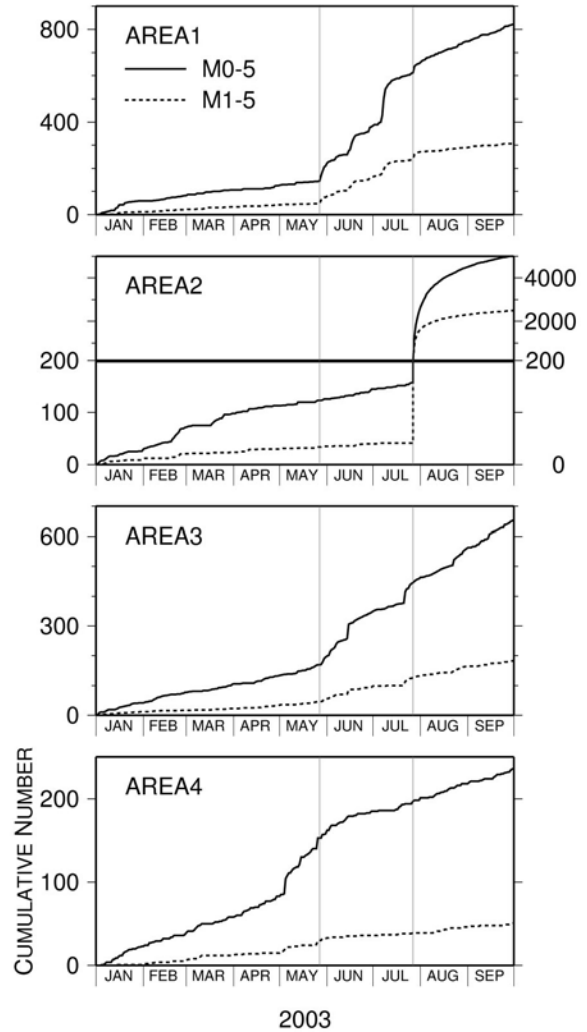

Fig. 2 Cumulative numbers of shallow earthquakes (depth ≤ 20 km) in AREA1 to 4, as indicated in Fig. 1. The numbers of the earthquakes of M0 to 5 is shown in solid lines and M1-5 in broken lines. May 26 and July 26, when large earthquakes occurred, are indicated by vertical lines.

Figure 1 shows the z-value and the ΔCFF for two possible orientations of the faults of the triggered seismicity. Both orientations have NS strikes with the first type having eastward dipping faults and the second type having westward dipping faults. Bright regions indicate areas where post-seismic seismicity becomes higher than pre-seismic seismicity. We can

see the increases of seismicity in AREA1 and AREA3, and the cumulative number of earthquakes (Fig. 2) also reflects the increases. We do not use any de-clustering algorithms in analyzing the background seismicity, because this method could cause loss of information of the events we are studying. In AREA1, the values for ΔCFF are positive (0.001 to 0.007 MPa) both in Figs. 1a and 1b. In AREA2, the z-value is almost zero indicating that the seismicity barely changed in the two months after the earthquake. This region includes hypocenters of a sequence of moderate earthquakes (M_{JMA} 5.6, 6.2, 5.4) on July 26, 2003, of which mechanisms are close

to supposed one (Fig. 1b). The ΔCFF values near the hypocenters have positive value of about 0.003 to 0.005 MPa in Fig. 1b. However, the high gradient for the ΔCFF values means that small changes of fault parameters could result in different ΔCFF values. AREA3 includes the locally highest ΔCFF value of about 0.01 MPa. Around the region with much lower z-values in the center of AREA3, the ΔCFF values are 0.005 to 0.008 MPa in Fig. 1a and 0.005 to 0.01 MPa in Fig. 1b. AREA4 has positive z-values, however Fig. 2 indicates that this could be caused by the events that occurred in early May.
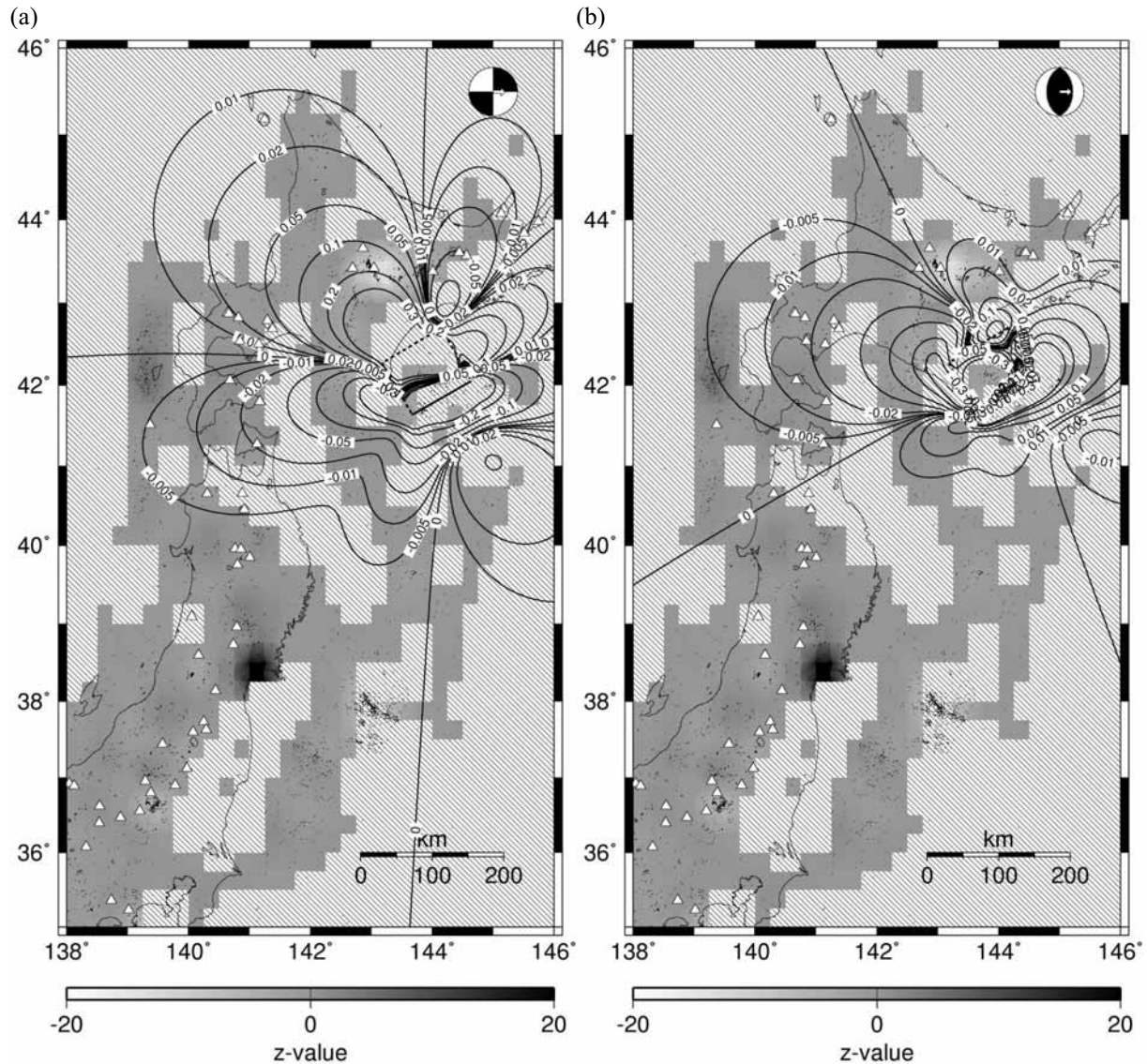

Fig. 3 Z-value and ΔCFF value. Z-values are estimated from shallow earthquakes (depth $\leq$ 20 km) of magnitude 0 to 5. Rectangular is the fault plane of the 2003 Tokachi-oki earthquake. The pre- and post-seismic periods are Jul 27 to Sep 25 and Sep 26 to Nov 25. Triangles are active volcanoes and dots are the hypocenters of the shallow earthquakes during the post-seismic period. Contour lines in (a) and (b) show the ΔCFF values in MPa calculated for a depth of 10 km, for two types of faults of the triggered seismicity. The types of faults are (a) EW right lateral and (b) NS strike with eastward dipping (45 deg), as illustrated by the stereoplots in the upper right of each figure. Absolute ΔCFF values larger than 0.3 MPa are clipped.

3 Detection and illustration of active response to teleseismic waves

When we study the active response to teleseisms, we can discount the possibility of the static influences. An effect of ΔCFF values is usually negligible because of small values much less than 0.01 MPa, which is thought to be required for the static triggering, by a few orders. Hence, we consider the possibilities of the dynamic triggering due to the teleseismic waves if the large earthquakes are far from Japan.

3.1 The 2003 Tokachi-oki earthquake

For this large earthquake of Mw 8.3 in Japan, we consider both static triggering within a few fault lengths from the main fault and dynamic triggering in main part of Japan.

(1) Seismicity changes

Figure 3 shows z-value for shallow earthquakes (depth ≤ 20 km) and ΔCFF for a depth of 10 km. To calculate z-values we use time-windows of 60 days before and after 26 September when the 2003 Tokachi-oki earthquake occurred. In the pre- and post-seismic periods, the analyzed earthquakes from JMA data have magnitudes of M0 to 5 and depths shallower than 20 km. We adopt the GSI model (CCEP, 2004) to calculate ΔCFF values as the previous section. We assume a simple rectangular fault plane (90 km × 92 km), where the slip is uniform, the eastern corner of the fault is located at 42.05N, 144.64E, the depth of the top of the fault is 15.7 km, strike = 241 deg, dip = 23 deg, rake = 124 deg, and slip = 4.84 m. The other parameters are the same as in the previous section. ΔCFF values are calculated for the faults with compressional mechanism due to the subduction of Pacific plate.

Negative z-values (increasing activities) are seen about 100 km NNW from the main fault, where ΔCFF values for EW right lateral fault have about 0.1 to 0.3 MPa (Fig. 3a) and those for NS reverse fault with eastern dipping about 0 to 0.02 MPa (Fig. 3b). The region includes active volcanoes; Tokachidake erupted in 1989 and Maruyama in 1898.

At the northern Miyagi regions where the sequence of moderate earthquakes (M_{JMA} 5.6, 6.2, 5.4) on July 26, 2003 occurred, ΔCFF values are scarcely changed while z-values there have large values because activities of the aftershocks are decreasing.

(2) Response to dynamic stress perturbations

To detect the active response to seismic waves from the 2003 Tokachi-oki earthquake, we use continuous velocity waveform data of Hi-net provided by NIED to look for high-frequency signals from possibly triggered small earthquakes. Observed high-frequency signals can be associated with sources in the crust or upper mantle in the vicinity of the observation station, however, these signals have to be distinguished from the seismic waves of the large mainshock. Generally, this can be done because at far distances the frequency content of seismic waves from the mainshock is different due to the loss of the high-frequencies from attenuation. We detect high frequency signals by the following process

[1] Filter the chosen velocity waveforms with a frequency pass-band of 5-20 Hz for each of three components (UD, NS, EW).
[2] Construct root-mean-square (RMS) envelopes of [1] with one second smoothing.
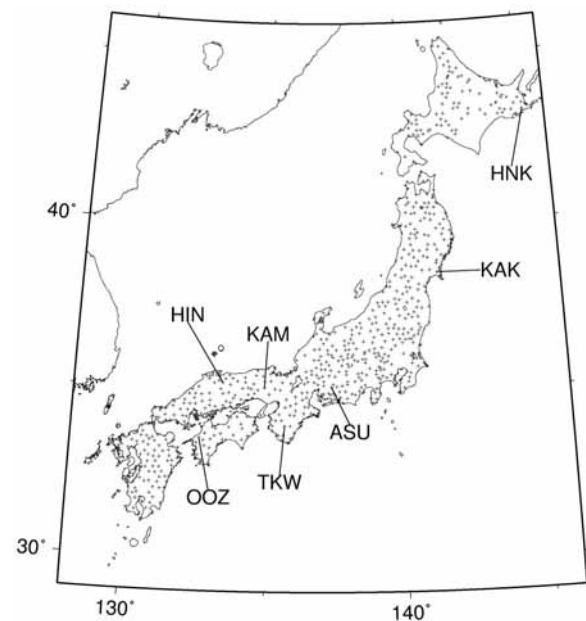[3] Calculate the z-value and statistic β value for amplitudes of the RMS envelopes.

Fig. 4 Hi-net observation stations. 642 stations analyzed in this study are indicated by crosses. In Fig. 6, RMS envelopes for the 7 labeled stations are shown.

Figure 4 shows the 642 observation stations used in this study. The RMS envelope constructed from three components of velocity waveforms, filtered with a pass-band of 5-20 Hz at station OOZ, is shown in Figs. 5 and 6. The station OOZ is located in western Shikoku, and the epicentral distance is about 1400 km. To illustrate that this envelope includes local events near the station and mainly excludes teleseismic waves, Fig. 5 compares the RMS envelope waveforms filtered with different pass-bands of 0.2-2, 2-5 and 5-20 Hz. The RMS envelope of 0.2-2 Hz shows both body waves followed by surface waves from the Tokachi-oki earthquake, while the envelope for 2-5 Hz shows mostly body waves (200-500 sec). Higher frequency components should include only direct body waves, because surface waves have longer period

components and scattered waves of the body waves in the coda are largely attenuated. However, the 5-20 Hz envelope includes energy around 400 sec, which is thought to be associated with local triggered events. These are also seen in the waveform filtered between 2-5 Hz.
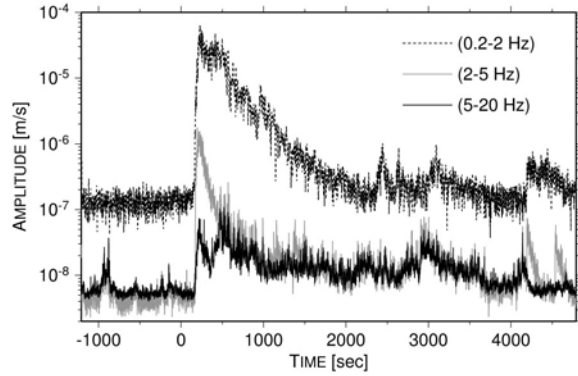

Fig. 5 RMS envelope waveforms filtered with pass-bands of 0.2-2, 2-5 and 5-20 Hz, at OOZ. Zero is the origin time of the 2003 Tokachi-oki earthquake (4:50'06 Sep 26, 2003 (JST)).
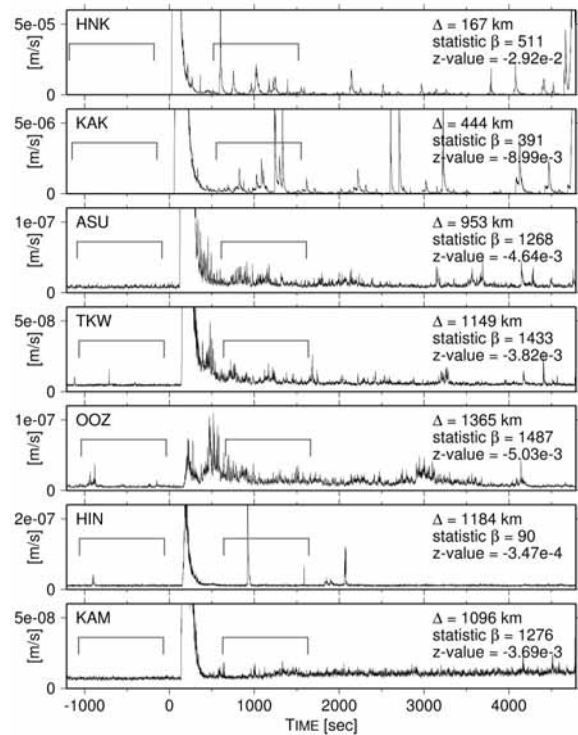

Fig. 6 RMS envelopes constructed from three component waveforms filtered with a pass-band of 5-20 Hz at HNK, KAK ASU, TKW, OOZ, HIN and KAM. The locations of the stations are shown in Fig. 4. Horizontal bars show the 1000 sec time windows for the pre- and post-seismic periods used for calculating z-values and statistic β values. Δ is hypocentral distance.

To statistically see changes of the envelope waveforms (5-20 Hz) we apply the z-value obtained by Eq. (2) for the amplitude of envelope waveforms instead of the number of events. The pre-seismic window is the 1000 sec up to the time ~200 sec before the arrival of the P wave. The post-seismic window is 1000 sec from ~500 sec after the arrival of the P wave (Fig. 6). In the previous section we calculated the z-values with a time unit of one day and here we use one second. Figure 7a illustrates the results of the z-value analysis for all of Japan. Low (negative) z-values are found around the Hokkaido and Tohoku regions, and are especially low on the Pacific side, indicating that aftershocks are included in the envelopes. The differences between the eastern and western regions of northern Honshu are due to a well-known difference in attenuation properties. Also the envelope from KAK may include continuing aftershocks of the events on 26 July. The western Shikoku, Kii peninsula, and the Tokai regions also have low z-values and observe swam-like tremor (Fig. 6). The tremor seems to have begun after the arrivals of the direct body waves and gradually disappeared in a few thousands of seconds. HIN is located in the vicinity of the fault of the western Tottori-ken earthquake in 2000, and observes one event in the post-seismic window.

Some positive and negative changes observed at only one station are sometimes local earthquakes or effects of the station due to noise. For example, a station KAM near the Yamasaki-fault shows a large negative z-value, while the surrounding stations show values of close to zero. Careful examination of the waveforms indicates that this was due to some noises after 5:00. We could not detect what are the sources of the noise, however this would not be related with the site effects because of no similar observations even in cases of the arrivals of the other teleseismic waves.

To reduce the influence of the aftershocks of the 2003 Tokachi-oki earthquake, we apply the statistic β value defined by Matthews and Reasenberg (1988) as

$$\beta = \left(n_2 - E(n_2)\right)/\sigma_2 \qquad (3)$$

where n_2 is the total number of earthquakes in the post-seismic term, $E(n_2)$ is the expected value estimated from the activity in the pre-seismic period, σ_2 is the standard deviation of the post-seismicity. A positive value indicates an increase of activity, and a negative value indicates a decrease. We use the amplitude of the envelope waveform as the number of events and obtain the statistic β value for the observed waves.

The statistic β value is based on a zero hypothesis that post-seismic activity is equal to the background with Poisson process, providing low absolute values in the regions influenced by the aftershocks because of large standard deviations.

Then the activity changes with small deviation are much cleared. We note that the statistic β value is very sensitive to noise perturbations. Hence, even though increasing activity (positive statistic β values) are dominantly found in Shikoku, Kii and Tokai (Fig. 7b), which is consistent with the negative z-values in these areas, we can not conclude whether the effect is due to natural events or noises.

For the three regions that show the high statistic β values and negative z-values, we calculate the correlation coefficients of envelope waveforms between the observation stations and a reference station in each region. The reference stations are OOZ, TKW and ASU, where the statistic β values are high and the z-values low compared with surrounding stations'. Contours in Figs. 7a and b show that similar envelope waveforms are observed over a wide area, therefore the increases of activity in those areas are not caused by local noises. Supposing a spherical and/or a cylindrical propagation of the signals (i.e. geometrical spreading), we can estimate the souses are approximately within a few tens of kilometers to 100 km from each reference stations. If the sources are in shallow region, much large increases of activity should be observed in contoured regions, which, however, are not found. Then they are caused by deep sources but not in shallow region.

Excitation of the tremor is especially strong in Shikoku among the three regions. The epicentral distance is more than 1400 km and the direct body waves are large attenuated and cannot be dominantly observed in very high frequency range. The excitation of the tremor appears to start from about 400 sec after the origin time of the earthquake, which is consistent with travel-times of S-waves and/or surface waves, although some similar tremor is also intermittently observed before that time (Figs. 5 and 6). It is difficult to determine the exact beginning of the excitation and whether it coincides with arrivals of the direct waves or later.

Figure 8 shows the hypocenters of earthquakes and deep low frequency (DLF) events in western Japan. The DLF events (M0 to 2) occur at depths of about 30 to 60 km on the subducting plate and have dominant frequencies of 1-10 Hz, while the ordinary earthquakes with the similar magnitudes have dominant frequencies of 10-20 Hz (Obara, 2003). Obara proposed that the DLF events are caused by fluid flow. The areas of small z-value and the large statistic β value seem to be coincident with the areas where DLF events are observed, suggesting the possibility that the swam-like tremor is excitation of DLF events.
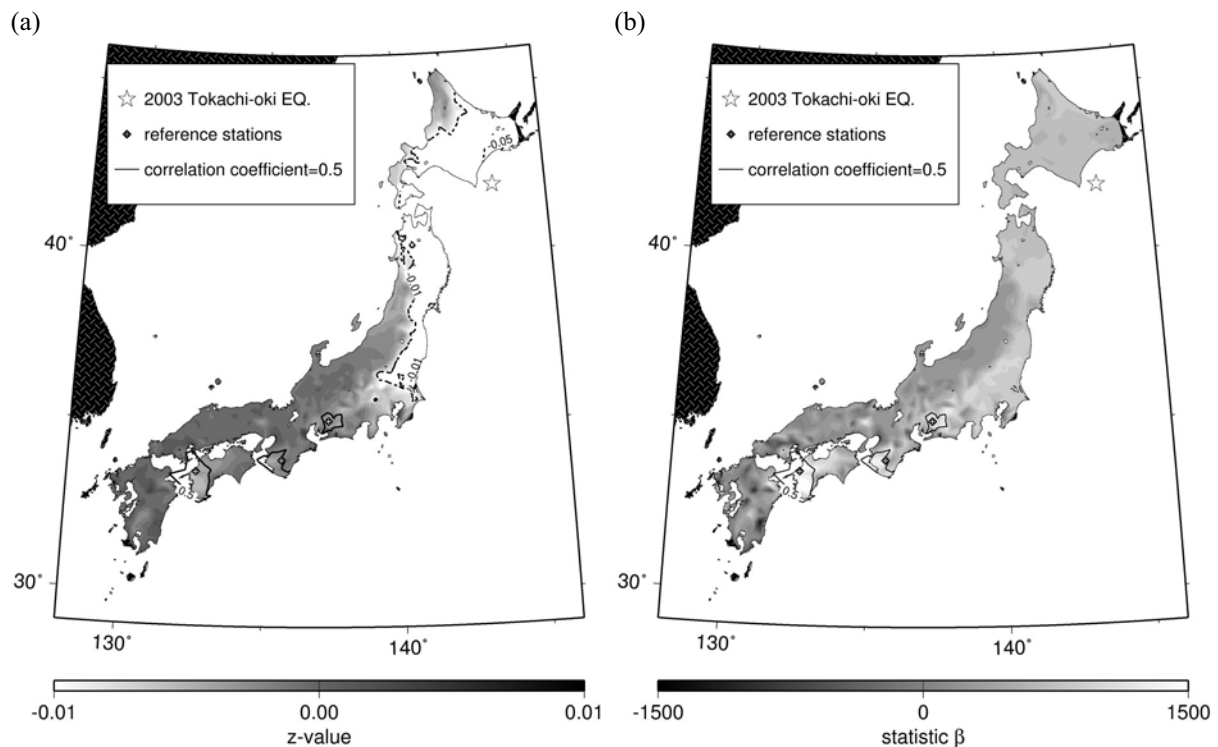

Fig. 7 Results showing the seismic amplitudes (5-20Hz) following the 2003 Tokachi-oki earthquake in Japan estimated by (a) z-value and (b) statistic β value. The white areas show where the mean amplitude of the RMS envelope after the arrivals of teleseismic waves is larger than before. Clipped values less than -0.01 in (a) are shown in broken lines. We contour with solid lines the regions where the RMS envelope waveforms have correlation coefficients larger than 0.5, with respect to reference stations. The reference stations are OOZ, TKW and ASU (see Fig. 4).
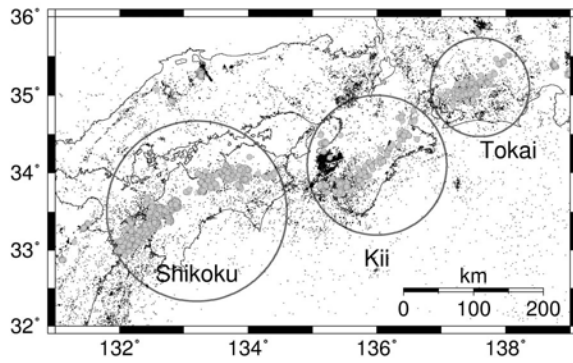
Fig. 8 Hypocenters of earthquakes and DLF events during 2003 (Jan to Dec) in western Japan. Dots are earthquakes and gray circles DLF events (M0 to 2).

3.2 Other teleseismic events

We investigate the active response to teleseismic waves from other earthquakes in 2003. We choose teleseisms, which occurred at night or in the early morning in Japan, in order to reduce cultural noise. Also, Hi-net records bore-hole data with generally low noise levels. We chose events with epicentral distances less than 8000 km and moment magnitudes (Mw) larger than about 7.0. We select nine earthquakes from the National Earthquake Information Center, U.S. Geological Survey, which are listed in Table 1, including the 2003 Miyagi-oki earthquake and the 2003 Tokachi-oki earthquake. The RMS envelopes at OOZ are shown in Fig. 9.

The swam-like tremor is not always observed in the Shikoku, Kii, and Tokai regions following these earthquakes, confirming that the inferred activity following the 2003 Tokachi-oki event cannot be attributed to stable site effects.

In Fig. 10 the DLF events in 2003 near Shikoku increase at the end of August around Bungo Strait and early in September around western Shikoku. Excitations of the tremor from the distant earthquakes were observed on September 26 and 27 in the Shikoku, Kii and Tokai regions, however, there was little change of earthquake activity. The excitation of tremor on September 27 starts from 1000 sec after the origin time and not at arrivals of the faster body waves.
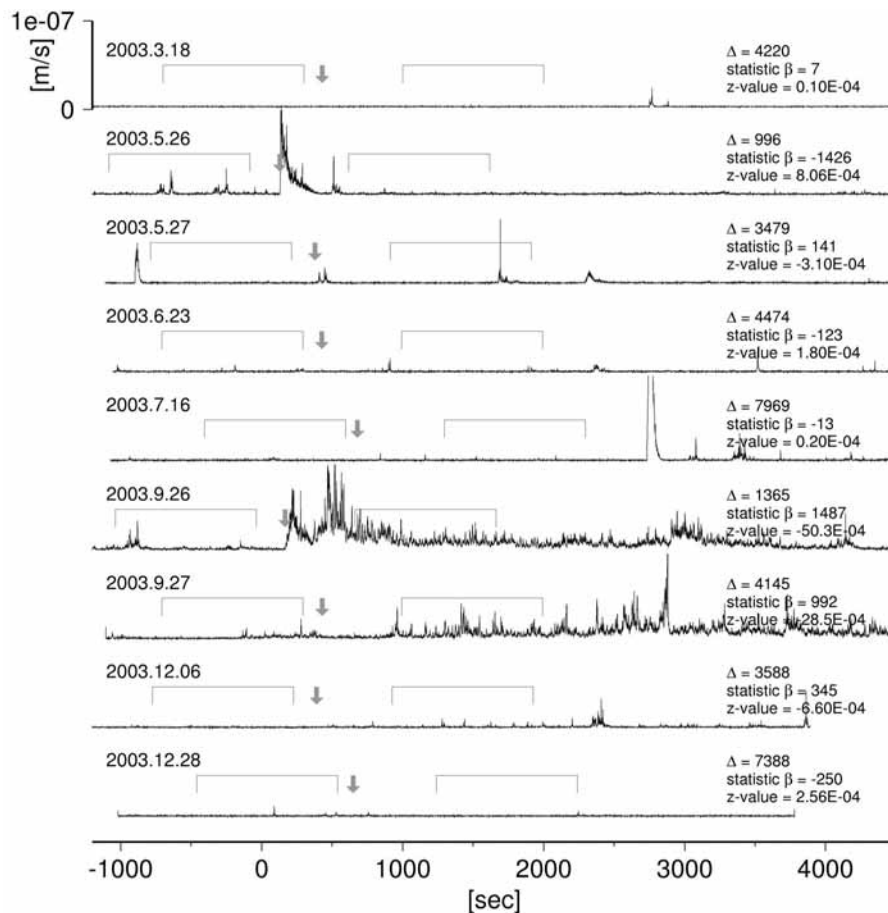

Fig. 9 RMS envelopes constructed from three component waveforms filtered with a pass-band of 5-20 Hz at OOZ. Zero indicates the origin time of earthquakes listed in Table 1. Horizontal bars show the 1000 sec time-windows used for calculating the statistic β value and z-value. The gray arrows indicate arrival times of the direct P-waves from the corresponding distant earthquake. Vertical scale, velocity, is common. For each event the epicentral distance Δ, statistic β value and z-value are indicated on the right.

Table 1 Teleseisms and large earthquakes in 2003

| Origin time and date (JST)	Latitude	Longitude	Depth (km)	Mw	Regional Location
Mar 18 01:36'17	51.272 N	177.978 E	33	7.0	Rat Islands, Aleutian Islands, Alaska.
May 26 18:24'33	38.849 N	141.568 E	68	7.0	Off coast of Miyagi prefecture, Japan.
May 27 04:23'28	2.354 N	128.855 E	31	7.0	Halmahera, Indonesia.
Jun 23 21:12'34	51.439 N	176.783 E	20	6.9	Rat Islands, Aleutian Islands, Alaska.
Jul 16 05:27'51	2.598 S	68.382 E	10	7.6	Carlsberg ridge.
Sep 26 04:50'06	41.815 N	143.910 E	27	8.3	Tokachi-oki, Japan.
Sep 27 20:33'25	50.038 N	87.813 E	16	7.3	Southwestern Siberia, Russia.
Dec 06 06:26'09	55.538 N	165.780 E	10	6.7	Komandorskiye Ostrova, Russia region.
Dec 28 01:00'59	22.015 S	169.766 E	10	7.3	Southeast of the Loyalty Islands.
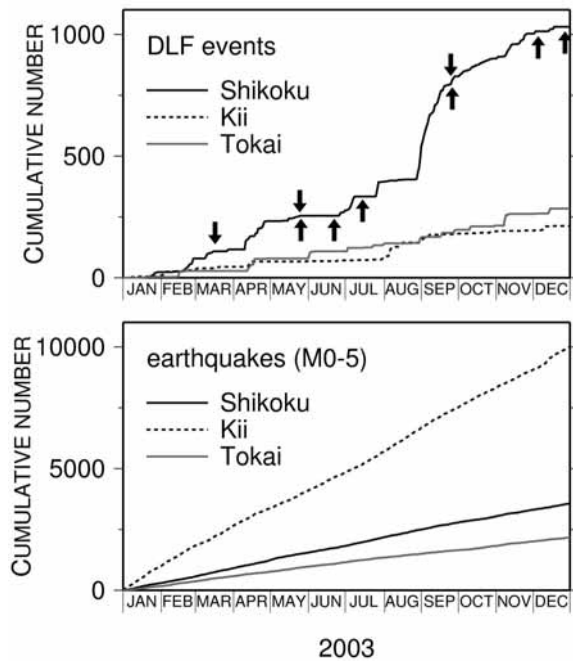
Fig. 10 Cumulative numbers of DLF events (M0-2) and earthquakes (M0 to 5) in the three areas of Shikoku, Kii and Tokai indicated in Fig. 8. The dates of occurrence of teleseisms in Table 1 are shown by the arrows.

4 Discussion and Conclusions

4.1 Triggered earthquakes in the Tohoku region due to the 2003 Miyagi-oki earthquake

In the region west of the earthquake where there was considerable seismic activity following the mainshock (AREA1 and AREA3 of Fig. 1) there were positive but small ΔCFF values (< 0.01 MPa), and it may be difficult to say that the events in this region were statically triggered. It is thought that static triggering requires changes of 0.01-0.1 MPa or greater. For these two regions, there is the possibility of dynamic triggering by the waves from the Miyagi-oki earthquake. The dynamic stress perturbations in AREA1 are order of 10^{-1} MPa, which would be thought to be much plausible reason than the static stress changes. The dynamic triggering does not involve a time-delay to excitation (Belardinelli et al., 2003) and the seismicity could increase immediately after the Miyagi-oki earthquake. Also, the areas include active volcanoes, which are susceptible to dynamic triggering, as reported by Hill et al. (1993) and Miyazawa (2002).

In and near the volcanic regions the mechanisms of earthquakes, for which ΔCFF is evaluated, are not always consistent with the supposed types. However it was difficult for ΔCFF to exceed 0.01 MPa in these regions, even if various mechanisms are chosen.

There was stable seismicity (no increases) in AREA2 to the southwest for two months following the mainshock, in an area where there were increases in the ΔCFF values, and then a sequence of moderate earthquakes occurred on July 26. If the values had major influence on the occurrences, this might have been an example of a delayed triggering due to static stress changes (Roy and Marone, 1996; Belardinelli et al., 2003). We actually provided information about this one week before the northern Miyagi earthquakes in July. Even if we could confirm that the triggering after May 26 is due to static stress changes and that time-delayed earthquakes might occur in areas of large ΔCFF values but low triggered seismicity, it is still difficult to predict the magnitude of the events (Dieterich, 1994).

In AREA1-3, ΔCFF values were small for the static triggering, however the increases of seismicity were observed in the western part of mainshock, where the ΔCFF values were positive. Or our results may show the possibility of the static triggering even with the order of 10^{-3} MPa one order smaller than it has ever been thought, which is still larger than the earth tide by 1-2 orders.

4.2 Seismicity after the 2003 Tokachi-oki earthquake

Seismic activity increased around volcanic regions in the center area of Hokkaido after the 2003 Tokachi-oki earthquake. These events would be triggered, however there are some possible reasons. One is the static triggering, because ΔCFF values were larger than 0.1 MPa, if the triggered earthquakes had mechanisms being close to supposed

NW-SE compression. We only consider the static changes due to the main event, however we cannot discount the coseismic slip with a large magnitude (> Mw 7.5) in one month after the mainshock. Also there is the possibility of dynamic triggering due to the seismic waves.

4.3 Dynamic triggering by the 2003 Tokachi-oki earthquake

Some observed active responses to the seismic waves of the Tokachi-oki mainshock could be attributed to dynamic triggering of small earthquakes.

Stations KAK and HIN showed large seismic amplitudes following the mainshock, however this may be due to coincidence and not a result of dynamic triggering. Both stations are close to the aftershock areas of recent earthquakes. KAK is close the 2003 Northern Miyagi sequence and HIN is close to the 2000 western Tottori earthquake (Mw 6.6). In areas of recent aftershocks, where the seismicity rate is relatively high, it is likely that small earthquakes occurred by chance during the 1000 seconds following the Tokachi-oki mainshock.

However, the excitation of the tremor observed on September 26 and 27 around the Shikoku, Kii, and Tokai regions is thought to be dynamic triggering due to seismic waves, probably S-waves and/or surface waves. The evidences from our analyses are as follows;

[1] The sources of the tremor are not in the immediate vicinity of one station but occur in some deeper regions around the slab, as inferred from the similar shape of RMS envelopes at different stations over wide area.

[2] Observed waves of this frequency range (5-20 Hz) are generally attributed to DLF events.

[3] The excitation appears to begin after arrivals of seismic waves with apparent velocities of 3-4 km/s, which are S-waves and surface waves.

Ukawa et al. (2002) argued that surface waves from shallow earthquakes tended to trigger local earthquakes in volcanic regions. Voisin (2002) numerically showed that, not only large amplitudes, but also low frequencies, such as surface waves, were likely to exceed the threshold for starting a rupture. Another possibility is that the triggering is caused by yield stress drops to the initial stress (Kilb et al., 2000), by cyclic fatigue on the fault (Gomberg et al., 2001). The stress perturbation at OOZ from the 2003 Tokachi-oki earthquake was on the order of 10^{-3} MPa, which would be too small to directly exceed the threshold for triggering events for each pulse of the seismic waves. DLF events are caused by fluid flows (Obara, 2002) and the triggering mechanism may be different from ordinary earthquakes, however they may be strongly influenced by the long period S- and/or surface waves. The faster body waves, P-waves, seem not to trigger the tremor, because the dynamic triggering involves instantaneous failures without a significant time delay (Belardinelli et al., 2003) and the excitation did not start immediately from the arrivals of those waves. Once triggered the tremor it seems to continue even without enough external dynamic perturbations of stress.

The high activity of DLF events for the active response under Shikoku (Fig. 10) is plausibly explained if they can be easily excited by the 2003 Tokachi-oki earthquake and later teleseisms. Also the activity seems to be related to the slow slip event (Mw 6.9) beneath Bungo Strait, west of Shikoku, which occurred from June to November in 2003. This suggests that dynamic triggering is related to not only high seismicity but also activity in the subduction zone. However, the excitation is also observed in other regions, Kii and Tokai, so the relationship between the dynamic triggering and the activity of the subduction zone is not well understood. We, however, note the excitation at Shikoku is significant.

The observation of the excited tremor only in September may be due to the large size of the waves from the 2003 Tokachi-oki earthquake. The seismic waves have the largest amplitudes and long period components that might be enough to trigger the events. The tremor sources may then become unstable and very sensitive to external perturbations for a certain time because of the fluid flow. Hence the next teleseism could trigger the same events even with small perturbations.

The mapping of z-values and statistic β values of observed envelopes following large earthquakes may provide a way to monitor the activity of the crust and upper mantle including the subduction zone, in regions where large earthquakes may occur in the future, although application of this monitoring to active faults is not presently possible, because of poor coverage of observation stations in local scale. Challenges for the future include the investigation of the mechanisms of dynamic triggering, understanding the relationship between dynamic triggering and the activity of the crust and the subduction zone, resolution of the source depth of the active responses, and the separation of the active response from other events, such as random coincidences and noise.

References

Belardinelli, M. E., Bizzarri, A. and Cocco, M. (2003): Earthquake triggering by static and dynamic stress changes, *J. Geophys. Res.* Vol. 108, 2135, doi:10.1029/2002JB001779.

The coordinating committee for earthquake prediction Japan (CCEP) (2004): *Report of the coordinating committee for earthquake prediction*, Vol. 71.

Dieterich, J. (1994): A constitutive law for rate of earthquake production and its application to earthquake clustering, *J. Geophys. Res.* Vol. 99, pp. 2601-2618.

Gomberg, J., Reasenberg, P. A., Bodin, P. and Harris, R. A. (2001): Earthquake triggering by seismic waves following the Landers and Hector Mine earthquakes, *Nature*, Vol. 411, pp. 462-466.

Habermann, R. E. (1983): Teleseismic detection in the Aleutian Island Arc., *J. Geophys. Res.* Vol. 88, pp. 5056-5064.

Harris, R. A. (1998): Introduction to special section: Stress triggers, stress shadows, and implications for seismic hazard, *J. Geophys. Res.*, Vol. 103, pp. 24347-24358.

Hashimoto, M. (1995): Static stress changes associated with the Kobe earthquake: calculation of changes in Coulomb failure function and comparison with seismicity change, *J. Seismol. Soc. Jpn.* Vol. 48, pp. 521-530. (abstract in English)

Hill, D. P., Reasenberg, P. A., Michael, A., Arabaz, W. J., Beroza, G., Brumbaugh, D., Brune, J. N., Castro, R., Davis, S., dePolo, D., Ellsworth, W. L., Gomberg, J., Harmsen, S., House, L., Jackson, S. M., Johnston, M. J. S., Jones, L., Keller, R., Malone, S., Munguia, L., Naba, S., Pechmann, J. C., Sanford, A., Simpson, R. W., Smith, R. B., Stark, M., Stickney, M., Vidal, A., Walter, S., Wong, V. and Zollweg, J. (1993): Seismicity remotely triggered by the magnitude 7.3 Landers, California, earthquake, *Science*, Vol. 260, pp. 1617-1623.

Kilb, D., Gomberg, J. and Bodin, P. (2000): Triggering of earthquake aftershocks by dynamic stresses, *Nature*, Vol. 408, pp. 570-574.

Matthews, M. V. and Reasenberg, P. A. (1988): Statistical methods for investigating quiescence and other temporal seismicity patterns, *PAGEOPH*, Vol. 126, pp. 357-372.

Miyazawa, M. (2002): *Scattering problems of seismic waves in passive and active structures*, Doctoral thesis, Kyoto University. (in Japanese)

National Earthquake Information Center, U. S. Geological Survey: http://neic.usgs.gov/

Obara, K. (2002): Nonvolcanic deep tremor associated with subduction in southwest Japan, *Science*, Vol. 296, pp. 1679-1981.

Okada (1992): Internal deformation due to shear and tensile faults in a half-space, *Bull. Seism. Soc. Am.* Vol. 82, pp. 1018-1040.

Reasenberg. P. A. and Simpson, R. W. (1992): Response of regional seismicity to the static stress change produced by the Loma Prieta earthquake, *Science*, Vol. 255, pp. 1687-1690.

Roy, M. and Marone, C. (1996): Earthquake nucleation on model faults with rate- and state-dependent friction: Effects of inertia, *J. Geophys. Res.*, Vol. 101, 13 919-13 932.

Toda, S., Tsuruoka, H. and Stein, R. S. (2001): Delayed but vigorous off-fault aftershocks triggered by the 6 October 2000 M=7.3 Tottori-ken-Seibu earthquake, Japan as a test of rate/state friction, *Seism. Res. Lett.*, Vol. 72, pp. 252.

Ukawa, M., Fujita, E. and Kumagai, T. (2002): Remote triggering of microearthquakes at the Iwo-jima volcano, *J. Geography*, Vol. 111, pp. 277-286 (abstract in English).

Voisin, C. (2002): Dynamic triggering of earthquakes: The nonlinear slip-dependent friction case, *J. Geophys. Res.*, Vol. 107, doi:10.1029/2001JB001121.

要 旨

　日本下の地殻と上部マントルの状態をモニタリングするために，我々は2003年に起きた規模の大きな地震に対する応答を調べた。5月26日の宮城県沖の地震(Mw 7.0)は，静的応力擾乱により東北地方で局地地震を誘発した。9月26日の2003年十勝沖地震(Mw 8.3)は，北海道中央部の浅部地震を静的に誘発し，1000 km以上離れた深部低周波微動を動的に誘発した。我々は能動的応答を図示するために，Hi-netの観測点で観測された地震波に対し，z値と統計的β値を用いた地震学的手法を提案する。

キーワード: 能動的応答，動的誘発，静的誘発，2003年十勝沖地震

日本列島下における活動的地殻の遠地地震波を用いた地震学的モニタリング

○宮澤　理稔・James J. Mori

１．はじめに

　近年微小地震観測網が全国的に整備され、インターネットを経由して地震波形記録が即時に得られるようになってきた。これらの記録を用いて、地震波に対する観測点近傍の構造の能動的応答を調べることで、日本列島直下の地殻と上部マントルの活動を準リアルタイムにモニタリングすることができる。〜10Hz に見られる活動が観測可能であり、GPS 等の測地学的手法に比べ十分短い時間スケールである。このような手法は或いは地震波に対する地震のダイナミックトリガリング（動的誘発）を調べることでもある。ダイナミックトリガリングとは対極的に、周波数のゼロ漸近による能動的応答として、スティックトリガリング（静的誘発）がある。これを調べる際は遅延時刻を考慮する必要があるので、気象庁一元化地震カタログを用いて地震活動を中心に解析する。このような誘発現象は地殻の活動状態を反映していると考えられるので、モニタリングのために重要である。本研究では 2003 年の解析結果を報告する。

２．遠地地震波に対する動的応答の検出

　地殻と上部マントルの能動的応答を調べるために、遠地地震波の入射を仮定する。ここに含まれる短周期の波は伝播過程で減衰するために、主に長周期の波の入射が期待できるので、観測波形にハイパスフィルターを施せば、遠地地震波ではない観測点近傍から輻射された波のみを抽出することができる。遠地地震到達前後における速度波形の RMS エンベロープの振幅を統計的に比較することで、能動的応答を評価する。防災科学技術研究所より整備提供されている Hi-net の、700 点近くの観測点での三成分連続速度波形記録を利用する。統計的評価の指標として、観測された速度記録に 5-20Hz のバンドパスフィルタを施した RMS エンベロープ波形の、地震波到達時前後 1000 秒の振幅に対し、z 値及び statistic β を計算する。z 値が小さい(負値)ほど、或いは statistic β が大きい(正値)ほど、地震波到達後のエンベロープ振幅が大きくなる。前者はパルス的な波形、後者は断続的な波形の検出が可能である。Hi-net の記録の得

られるすべての観測点について、これらの値を求めることで、北海道から鹿児島までの日本列島における能動的或いは受動的応答の様子を示すことができる。

　2003 年十勝沖地震に伴う地震波を用いた解析を行ったところ、北海道から東北地方の太平洋側に z 値の小さな領域が認められた。これは異常震域に沿った領域で、余震がよく観測されたことを意味する。statistic β は震央から 1000 km 以上も離れた東海地方、紀伊半島、四国に大きな値が得られた。観測点間で観測波形の相関を取ることで、局所的な活動やノイズでないことが分かった。これらは深さ 30-60 km 程度のプレート境界付近で発生する深部低周波微動であると考えられる。つまり十勝沖地震によって深部低周波微動が誘発された可能性がある。

３．静的応力場変化に対する地震活動

　5 月 26 日の宮城県沖の地震($\text{M}_{\text{JMA}}7.1$)前後 2 ヶ月間の、同地方の地震活動度の変化を z 値として計算した。内陸部の深さ 20 km 以上の浅部で明瞭な地震活動の増加が認められた。この地域は宮城県沖の地震に対する ΔCFF(但し二次的震源を南北方向に走行を持つ逆断層と仮定)と正の相関があるが、ややΔCFF 値が小さいのでダイナミックトリガリングの可能性もある。

　ΔCFF がより大きな値を持つにも関わらず、地震の活動の増加が殆ど認められなかった地域がある。これは 2 ヶ月後の 7 月 26 日に宮城県北部で、一連の地震活動(M $_{\text{JMA}}$ 5.6, 6.2, 5.4)があった地域を含む。スタティックトリガリングはダイナミックトリガリングとは異なり、破壊遅延を有することがある。従って、これらの一連の活動は 5 月 26 日の地震によって静的に誘発された可能性がある。